

SOFC-anodes, proof for a finite-length type Gerischer impedance?

B.A. Boukamp^{a,*}, M. Verbraeken^a, D.H.A. Blank^a, P. Holtappels^b

^a *Inorganic Materials Science, Faculty of Science and Technology and MESA+ Institute for Nano Technology, University of Twente, P.O. Box 217, Enschede 7500 AE, The Netherlands*

^b *Laboratory for High Performance Ceramics, EMPA Materials Science and Technology, Überlandstr 129, CH-8600 Dübendorf, Switzerland*

Received 29 June 2005; received in revised form 27 February 2006; accepted 1 March 2006

Abstract

The impedance of a symmetric cell with Ni/Ti-doped YSZ cermet anodes was measured as function of ambient (P_{H_2} , P_{H_2O}) and temperature. The impedances showed identical shapes with a minor dispersive contribution in the high frequency region and a dominating dispersion down to 0.01 Hz. The characteristic shape of this dispersion was clearly in between a finite-length Warburg (FLW) and a Gerischer impedance. Analysis of the dispersion in the Bode representation, after subtraction of the high frequency contribution, showed a clear relation with the Gerischer impedance. Assuming a finite-length constraint led to quite reasonable modelling of the data. The parameter set of this finite-length Gerischer showed a consistent dependence on P_{H_2} , P_{H_2O} . A qualitative interpretation of this modified Gerischer is presented.
© 2006 Elsevier B.V. All rights reserved.

Keywords: SOFC; Cermet anodes; Impedance analysis; Finite-length Gerischer

1. Introduction

Analysis of the impedance spectra of porous SOFC-electrodes is often quite complicated. The relation between the so-called equivalent circuit elements and actual physical transport and transfer processes remains often vague. Exceptions are the perovskite-type cobaltate–ferrite cathodes, which can be modelled with a Gerischer impedance [1]. The Gerischer response has been derived for a CEC type electrochemical reaction in a liquid electrolyte [2,3]. But the actual proof of the existence of this Gerischer impedance was only observed much later and for non-aqueous systems [4]. The most direct derivation of the simplified Gerischer expression is by incorporating a ‘sink’ term in Fick’s second law, i.e. a local concentration change results in a, non-Faradaic, side reaction that affects the concentration, e.g. (see also Ref. [5]):

$$\frac{dc(x,t)}{dt} = \tilde{D} \frac{d^2c(x,t)}{dx^2} - k \cdot c(x,t) \quad (1)$$

where $c(x,t)$ is the concentration variation (excess concentration above the equilibrium concentration) and k is the reaction rate

under the assumption that the concentration of the reaction product can be considered constant. For semi-infinite diffusion with a side reaction the frequency domain solution of both Fick laws then follows as [5]:

$$Z(\omega) = \frac{Z_0}{\sqrt{\tilde{D} \cdot (k + j\omega)}} \quad (2)$$

One interpretation [1] is the competition between surface and bulk diffusion, which is coupled through the surface oxygen exchange process, see Fig. 1A. But also slow adsorption coupled with surface diffusion can yield a Gerischer response [6], see Fig. 1B.

Recently a ‘fractal’ Gerischer response was observed for chromate–titanate based porous SOFC-anodes [7]. The remarkable property of the Gerischer impedance is that it is based on semi-infinite diffusion, but results in a finite dc-value. In [5] a finite-length expression for a Gerischer was derived:

$$Z(\omega) = \frac{Z_0}{\sqrt{(k + j\omega) \cdot \tilde{D}}} \tanh \left[L \sqrt{(k + j\omega) / \tilde{D}} \right] \quad (3)$$

which reduces to the original Gerischer expression when it can be assumed that $\tilde{D} \ll L^2 \cdot k$. Current results on symmetric cells with

* Corresponding author.

E-mail address: b.a.boukamp@tnw.utwente.nl (B.A. Boukamp).

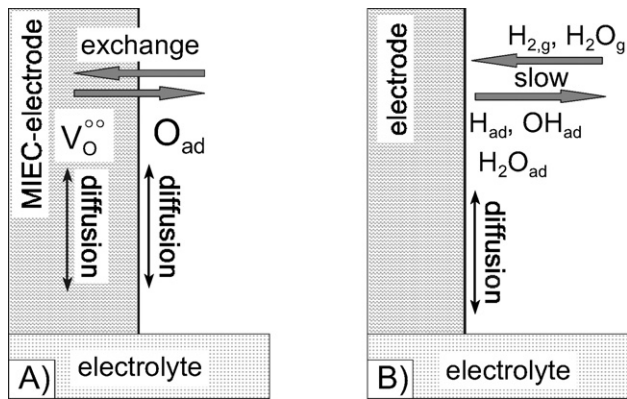


Fig. 1. Schematics of electrode reactions that can lead to a Gerischer response. A) The 'ALS' model [1], B) slow adsorption coupled to surface diffusion (Atangulov and Murygin [6]).

active porous Ti-doped YSZ/Ni anode layers seem to indicate the need for a finite-length Gerischer expression.

2. Experimental procedure

Symmetrical cells were prepared by EMPA [8] using dry-pressed NiO/YSZ cermet pellets as support. The active anode layer of a NiO/18% Ti-doped YSZ was added by spray deposition, followed by deposition of the YSZ electrolyte layer. By sintering two half cells together symmetrical cells were obtained with an electrode area of 1.27 cm². For further details see Ref. [8]. The cell impedance was measured with a Solartron 1255 FRA, coupled to a 1287 Electrochemical Interface, as function of P_{H_2}/P_{H_2O} . The temperature dependence will be presented in a separate paper [8]. Impedance data were validated with a Kramers–Kronig test procedure [9]. Initial data analysis was performed with the 'Equivalent Circuit' program [10], followed by a semi-graphical optimisation analysis with the Microsoft Excel™ spreadsheet program.

3. Results and discussion

3.1. Analysis and modelling procedure

An example of the cell impedance for several P_{H_2} values at 800 °C is presented in Fig. 2. Initial data analysis indicated a simple high frequency dispersion (CPE parallel to a small resistance), but the dominant low frequency dispersion could not be resolved satisfactorily with standard dispersive elements. Neither the finite-length Warburg (FLW) nor the Gerischer (even in a double-fractal form [7]) could approximate the measured dispersion adequately. For a more detailed analysis the high frequency section (~100 to 10 kHz) was modelled with a R(RQ) Q sub-circuit. Here the circuit description code developed by [10] is followed. Subsequently the R(RQ) dispersion is subtracted from the data and the reduced data set is analysed using a spreadsheet program. The Bode plot of Fig. 3 presents a typical example of the resulting low frequency dispersion.

Before further analysis, the reduced data set was tested for Kramers–Kronig compatibility [9]. The results, as shown in

Fig. 3, indicate high quality data. The imaginary part is characterized by a high frequency slope slightly larger than -0.5 , while the low frequency slope is somewhat lower than 1. The real part tends to a constant value for $\omega \rightarrow 0$. The high frequency slope is identical to the imaginary one. Although the observed shape suggests a Gerischer, even the double-fractal Gerischer [7] resulted in a poor match (see Fig. 4). Assuming that conditions could lead to a finite-length effect, i.e. \tilde{D} in the order of, or larger than $L^2 \cdot k$, the finite-length Gerischer expression (Eq. (3)), is tested here. Because the Bode plot slopes (Fig. 3) deviate from 1 (n) and -0.5 (α) a double-fractal expression was developed for Eq. (3):

$$Z_{FFLG}(\omega) = \frac{Z_0 \tanh\left(L[k + (j\omega)^n]^\alpha / \sqrt{\tilde{D}}\right)}{\sqrt{\tilde{D}}[k + (j\omega)^n]^\alpha} \quad (4)$$

The fractal expression in the argument can be developed as follows:

$$[k + (j\omega)^n]^\alpha = \left[k + \omega^n \cos \frac{n\pi}{2} + j\omega^n \sin \frac{n\pi}{2} \right]^\alpha = [a + jb]^\alpha \quad (5)$$

with:

$$(a + jb)^\alpha = \left\{ \cos \left[\alpha \cdot \tan^{-1} \left(\frac{b}{a} \right) \right] + j \sin \left[\alpha \cdot \tan^{-1} \left(\frac{b}{a} \right) \right] \right\} \times (a^2 + b^2)^{\alpha/2} \quad (6)$$

This results in a separated real and imaginary part for the tanh argument, $p + jq$. The tanh function can then also be separated into a real and imaginary part:

$$\tanh[p + jq] = \frac{\sinh(2p) + j \sin(2q)}{\cosh(2p) + \cos(2q)} \quad (7)$$

Subsequent combination of all these functions in the spreadsheet program allows the simulation of the double-fractal finite-length Gerischer function. In order to fit the FFL-Gerischer to the data set the n and α exponents were obtained from the slopes of the Bode representation (Fig. 3) and kept fixed in the fitting procedure. Although the match between model and data is still not optimal, it is a far better match than the modelling with the double-fractal Gerischer, as can be seen from Fig. 4, or the finite-length Warburg (FLW, not shown).

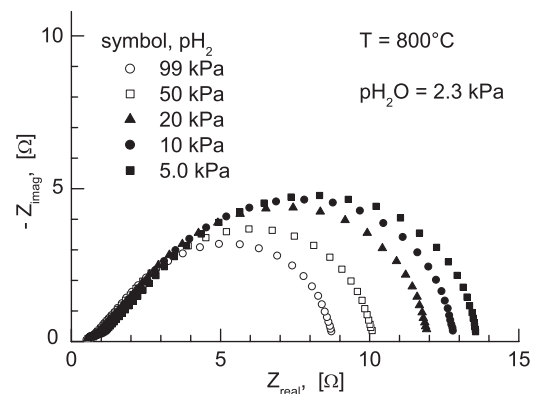


Fig. 2. Electrode impedances for a symmetric cell as function of P_{H_2O} . Electrode area is 1.27 cm² for each electrode.

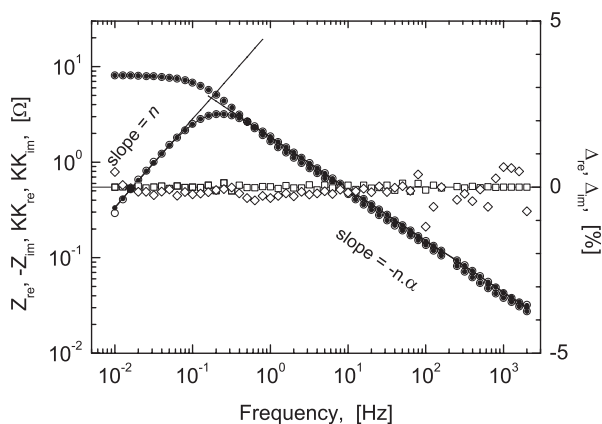


Fig. 3. Bode representation of the low frequency dispersion, after subtraction of the high frequency $R(RQ)$ contribution. Data: (●), Kramers–Kronig transform: (○). The residuals between the data and K–K transform are also presented (□, ◇, right hand axis).

3.2. Parameter dependence on P_{H_2} and P_{H_2O}

The impedances were measured as function of P_{H_2} and P_{H_2O} . This combination constitutes the local P_{O_2} , which is the key parameter for the electrochemical properties of the Ti-doped YSZ. The equivalent P_{O_2} was calculated using thermodynamic data from [11]. The adjustable parameters of the FFL-Gerischer model are presented in Fig. 5 as function of this equivalent P_{O_2} . This helps in distinguishing between surface adsorption and bulk effects. From Fig. 5 it seems that the reaction rate, k , is controlled by the Ti–YSZ bulk properties. An increase with increasing P_{O_2} is rather unexpected. One tentative explanation could be that the reaction rate k relates to the transfer of adsorbed oxygen species to the Ti–YSZ grain interior, e.g.:



The concentration of *free* vacancies is likely to *decrease* with *decreasing* P_{O_2} through the increase in Ti_{Zr} centres that can form immobile $[Ti_{Zr}-V_O]^{\bullet}$ complexes (in analogy with [6]). The contribution of oxygen (vacancy) transport through the Ti–YSZ

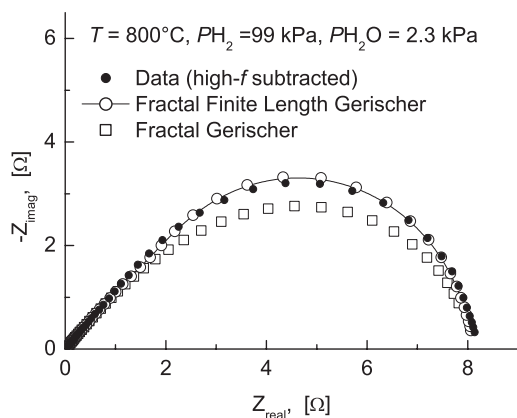


Fig. 4. Comparison between actual data set (high frequency contribution removed), the fractal-finite-length Gerischer and a simple fractal Gerischer response.

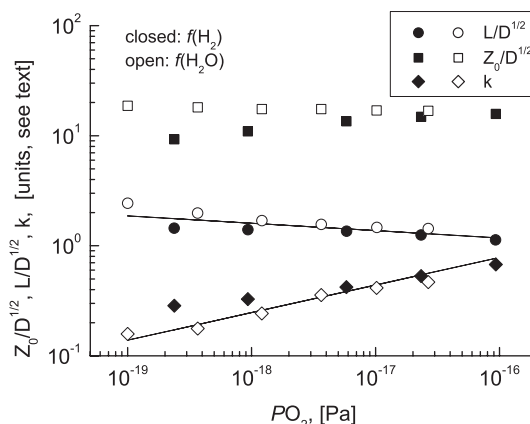


Fig. 5. Key parameters of the FFL-Gerischer at 800 °C, presented as function of the local P_{O_2} . Closed symbols: function of P_{H_2} at $P_{H_2O}=2.3$ kPa, open symbols: function of P_{H_2O} at $P_{H_2}=81$ kPa. The P_{O_2} is derived from the relation: $P_{O_2} = (P_{H_2O}/(P_{H_2} \times 10^{-(2.958-13022/T)}))^2$, where pressures are in atm [11].

grains is not significant, regarding the high dopant concentration. Hence it is assumed that surface diffusion to a triple phase boundary site is the dominant electrode process. The exchange of oxygen with the bulk, according to a scheme similar to Eq. (8), under influence of the ac-perturbation, is sufficient condition for the existence of a Gerischer response. An interesting parameter is the L/\sqrt{D} combination with an observed value of $\sim 1-3$ s^{1/2}. Assuming L to be in the order of the thickness of the active layer (~ 20 μm) this leads to a \bar{D} -value in the order of 10^{-6} cm²·s⁻¹, which seems quite reasonable for surface diffusion. Based on the ‘finite-length conditions’ the reaction rate should then be in the range $k \sim 0.25$ s⁻¹, as observed in Fig. 5. In case the Gerischer mechanism involves bulk diffusion, then a much shorter diffusion length, in the order of the grain size, should be assumed.

4. Conclusions

Careful impedance analysis, using a reduced data set, results in strong support for the existence of a finite-length Gerischer. Resulting fit parameters show consistent trends as function of the ambient P_{H_2} and P_{H_2O} . A tentative interpretation of the P_{O_2} dependence of the reaction constant, k , seems to point to the formation of immobile $[Ti_{Zr}-V_O]^{\bullet}$ complexes.

References

- [1] S.B. Adler, J.A. Lane, B.C.H. Steele, J. Elchem. Soc. 143 (1996) 3554.
- [2] H. Gerischer, Z. Phys. Chem. 198 (1951) 216.
- [3] M. Sluyters-Rehbach, J.H. Sluyters, in: E. Yeager, et al., (Eds.), Comprehensive Treatise of Electrochemistry, vol. 9, Plenum, New York, 1984, p. 274.
- [4] R.C. Makkus, K. Hemmes, J.H. de Wit, Ber. Bunsenges. Phys. Chem. 94 (1990) 847.
- [5] B.A. Boukamp, H.J.M. Bouwmeester, Solid State Ion. 157 (2003) 29.
- [6] R.U. Atagulov, I.V. Murugin, Solid State Ion. 67 (1993) 9.
- [7] M. González-Cuenca, W. Zipprich, B.A. Boukamp, G. Pudmich, F. Tietz, Fuel Cells 1 (2001) 256.
- [8] P. Holtappels, These proceedings.
- [9] B.A. Boukamp, J. Electrochem. Soc. 142 (1995) 1885.
- [10] B.A. Boukamp, Solid State Ion. 20 (1986) 31.
- [11] R. Hartung, H.-H. Möbius, Chemie-Ing. Techn. 40 (1968) 592.